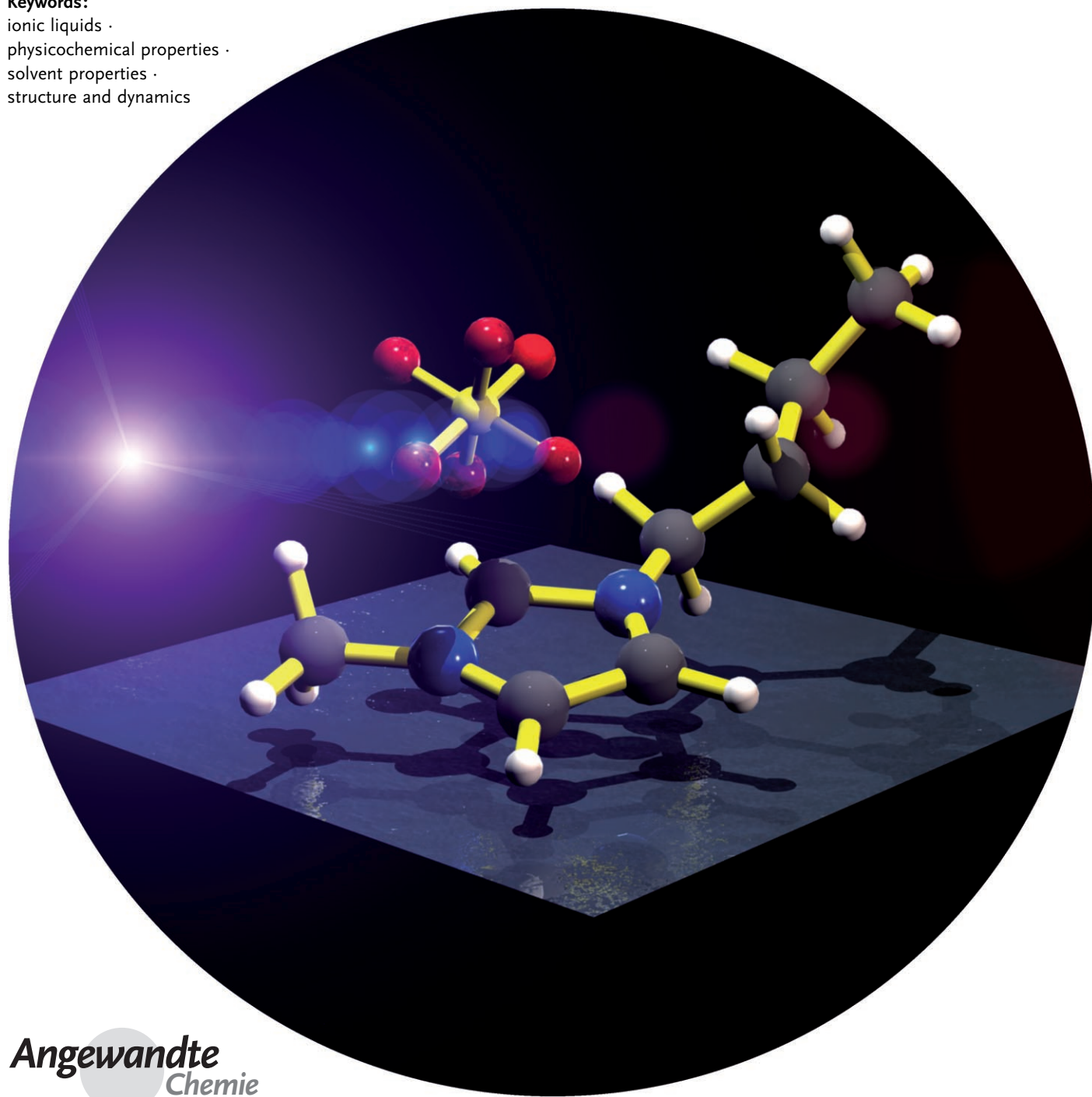


Understanding Ionic Liquids at the Molecular Level: Facts, Problems, and Controversies

Hermann Weingärtner*

Keywords:

ionic liquids ·
physicochemical properties ·
solvent properties ·
structure and dynamics



Ionic liquids (ILs) are organic salts with melting points near room temperature (or by convention below 100°C). Recently, their unique materials and solvent properties and the growing interest in a sustainable, “green” chemistry has led to an amazing increase in interest in such salts. A huge number of potential cation and anion families and their many substitution patterns allows the desired properties for specific applications to be selected. Because it is impossible to experimentally investigate even a small fraction of the potential cation–anion combinations, a molecular-based understanding of their properties is crucial. However, the unusual complexity of their intermolecular interactions renders molecular-based interpretations difficult, and gives rise to many controversies, speculations, and even myths about the properties that ILs allegedly possess. Herein the current knowledge about the molecular foundations of IL behavior is discussed.

1. Introduction

Simple inorganic salts, such as NaCl, melt at very high temperatures, which render their routine use as solvents for chemical processing impossible. Salts with organic cations open a window for the liquid state at more moderate temperatures. Adopting such ideas, the past decade has seen the advent of a new class of solvents, referred to as “ionic liquids” (ILs).^[1] This term describes organic salts that are liquid at or near room temperature, taking 100°C as an arbitrary upper limit.

The first report of a room-temperature molten salt, ethylammonium nitrate, goes back to 1914,^[2] but subsequently, it was not recognized that chemistry in such solvents could become of widespread interest. Organic chloroaluminates, first mentioned in 1951^[3] and studied in detail from the 1970s onwards,^[4] are now considered to form the first generation of ILs. However, owing to rapid hydrolysis, such salts require an inert-gas atmosphere. In the 1990s it became increasingly clear that many ion combinations form air- and water-stable ILs.^[5] Since then ILs have become increasingly popular in academia and industry. Because of their low volatility they are being explored as “green” substitutes for volatile organic solvents. Their unique properties favor applications in diverse fields, such as synthesis, catalysis, biocatalysis, separation technology, electrochemistry, analytical chemistry, and nanotechnology.^[1] The unique variability of the ions often allows the properties of interest to be imparted, so that ILs are denoted as “designer solvents”. For example, ILs may be strongly hydrophobic or hydrophilic, and may not even mix with one another.^[6] A molecular-based understanding of their properties should largely facilitate a rational design.

A molecular-based understanding is a great challenge because the charge and the molecular and electronic structure of the ions give rise to a complex interplay of molecular interactions. Moreover, theoretical analyses often have to be based on incomplete or uncertain experimental data. Many physicochemical properties are now well characterized and

available from public data bases, such as “ILThermo” managed by the U.S. National Institute of Standards and Technology. However, some experimental methods, which are readily applied to molecular liquids, are not easily conducted with ILs or are even infeasible. Moreover, some well-established rules and correlations for assessing the properties of molecular liquids are not easily transferred to ILs. Altogether, this situation has given rise to controversies, speculations, and even myths about the properties of ILs.

The aim of this Review is to describe the molecular foundations of IL behavior. To keep the length manageable, the Review is highly selective and focuses on major developments, open problems, and current controversies. In Section 2 there is a discussion of the intermolecular forces and the resulting structure of ILs. Section 3 gives a summary of the current knowledge concerning molecular motions in ILs. In Sections 4 and 5, respectively, the bulk physical properties and solvent behavior of ILs are considered.

2. The Structure of Ionic Liquids

2.1. The Ionic Constituents

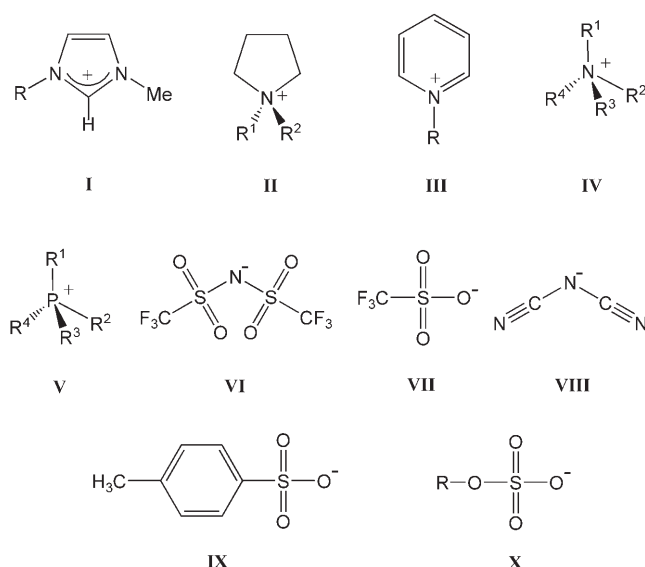
2.1.1. Representative Ions

Scheme 1 defines some important ions and introduces their abbreviations. Apart from the widely employed 1-alkyl-3-methylimidazolium ions (**I**), the most preferred salts are those with pyrrolidinium (**II**), pyridinium (**III**), tetraalkylammonium (**IV**), or tetraalkylphosphonium ions (**V**). There is now also an increasing interest in cations with functionalized, for example, polar, fluorinated, or chiral side chains which are

From the Contents

1. Introduction	655
2. The Structure of Ionic Liquids	655
3. Molecular Motions in Ionic Liquids	660
4. Macroscopic Properties of Ionic Liquids	662
5. Solvent Properties of Ionic Liquids	665
6. Conclusions	668

[*] Prof. Dr. H. Weingärtner
Physical Chemistry II
Ruhr-University of Bochum
44780 Bochum (Germany)
Fax: (+49) 234-32-14293
E-mail: hermann.weingaertner@rub.de



Scheme 1. Important ions: **I**: 1-alkyl-3-methylimidazolium ($[C_n\text{mim}]^+$, C_n stands for n -alkyl residues C_nH_{n+1}); **II**: 1,1-dialkylpyrrolidinium ($[C_mC_n\text{pyr}]^+$); **III**: 1-alkylpyridinium ($[C_n\text{py}]^+$); **IV**: tetraalkylammonium ($[N_{ijkl}]^+$); **V**: tetraalkylphosphonium ($[P_{ijkl}]^+$); **VI**: bis(trifluoromethanesulfonyl)amide ($[\text{Tf}_2\text{N}]^-$); **VII**: trifluoromethanesulfonate ($[\text{TfO}]^-$); **VIII**: dicyanamide ($[(\text{CN})_2\text{N}]^-$); **IX**: tosylate ($[\text{OTos}]^-$); **X**: alkylsulfates ($[C_n\text{OSO}_3]^-$).

often optimized for given applications. Such ILs are usually denoted as “task-specific ionic liquids”. The physical properties of this new generation of ILs are, however, more-or-less unexplored.

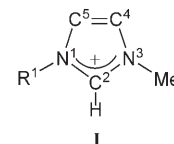
Among the anions, halides give rise to unfavorable properties and are strongly hygroscopic. Much work has focused on salts based on $[\text{BF}_4]^-$ or $[\text{PF}_6]^-$ ions, but in the presence of moisture these anions hydrolyze, forming HF among other things.^[7] More complex perfluorated anions,^[5b,e] such as bis(trifluoromethanesulfonyl)amide ($[\text{Tf}_2\text{N}]^-$) (**VI**) or trifluoromethanesulfonate ($[\text{TfO}]^-$) (**VII**), or halogen-free ions, such as dicyanamide (**VIII**), tosylate (**IX**), or n -alkylsulfates (**X**), are now preferred.^[1c] In particular, $[\text{Tf}_2\text{N}]^-$ (**VI**) forms liquid salts of low viscosity with high thermal and electrochemical stability.^[5e] If $[\text{Tf}_2\text{N}]^-$ is replaced by its non-fluorinated homologue, bis(methanesulfonyl)amide, there is a notable rise in viscosity and a decrease in thermal and electrochemical stability,^[8] highlighting the advantages of perfluorated anions.



Hermann Weingärtner was born in 1948 in Offenburg. He received his doctorate in 1976 for work carried out in the group of H. G. Hertz in Karlsruhe on nuclear magnetic resonance in electrolyte solutions. After his “Habilitation” in 1986 and after several research fellowships, among others at the Australian National University in Canberra, he was appointed, in 1995, to a professorship for Physical Chemistry at the Ruhr-University of Bochum. His major scientific activities are in the field of thermophysical properties of fluids.

2.1.2. Peculiarities of Imidazolium Salts

Among the various IL families 1-alkyl-3-methylimidazolium salts exhibit unique properties which are founded in the electronic structure of the aromatic cations (Scheme 2). This electronic structure is best described as comprising a delocalized 3-center-4-electron configuration across the N1-C2-N3 moiety, a double bond between C4 and C5 at the opposite side of the ring, and a weak delocalization in the central region.^[9] The hydrogen atoms C2-H, C4-H, and C5-H carry almost the same charge, but carbon C2 is positively charged owing to the electron deficit in the C=N bond, whereas C4 and C5 are practically neutral. The resulting acidity of the hydrogen atoms is the key to understanding of the properties of these salts.^[9]

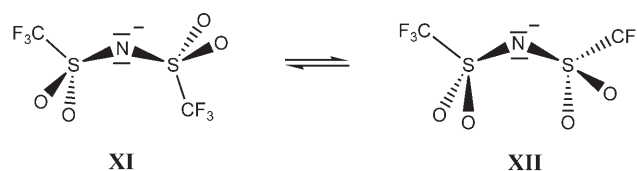


Scheme 2. Denotation and electronic structure of 1-alkyl-3-methylimidazolium ions.

2.1.3. Conformational Equilibria

In cations, torsional motions of the alkyl groups can give rise to conformational equilibria. For example, *trans-trans*- and *trans-gauche*-conformations of the n -butyl chain in $[C_4\text{mim}]^+$ result in different crystalline polymorphs.^[10] It is likely that the coexistence of these conformers significantly affects the liquid structure and has far-reaching consequences on the bulk properties of ILs. Hamaguchi and Ozawa^[10d] have argued that this structure-conformational heterogeneity may even result in nanostructured fluids.

An example for conformational equilibria of anions is $[\text{Tf}_2\text{N}]^-$, which forms *trans*- and *cis* conformers (Scheme 3). In



Scheme 3. Conformational equilibrium of the $[\text{Tf}_2\text{N}]^-$ ion (**VI**) with the two CF_3 groups *trans* (**XI**) and *cis* (**XII**) to one another.

liquid $[C_1\text{mim}][\text{Tf}_2\text{N}]$ the *trans* form (**XI**) prevails,^[11] whereas in the crystal structure the *cis* conformer (**XII**) is found.^[12] The different steric and electronic environments of the two conformers are thought have major consequences for the bulk properties of these salts, and may rationalize their low melting points and low viscosities.

2.2. Ionic Interactions

The molecular interactions between ions result from their geometry and charge distribution. In simple salts the interactions are controlled by long-range Coulomb forces between the net charges of the ions. With molecular ions their bulky

size and asymmetric charge distribution softens the Coulomb forces and generates highly directional interactions of shorter range. The interaction potential [Eq. (1)] depends on the distance r of the ions and a set of angles Ω for their mutual orientation. It comprises terms for electrostatic (U_{es}), inductive (U_{ind}), and van der Waals (dispersive/repulsive) interactions (U_{vdW}).

$$U(r, \Omega) = U_{\text{es}}(r, \Omega) + U_{\text{ind}}(r, \Omega) + U_{\text{vdW}}(r, \Omega) \quad (1)$$

Equation (1) is often supplemented by terms for specific interactions, for example, interactions between the π -systems of aromatic rings or hydrogen bonds. For example, hydrogen bonds may be relevant for the structure of neat ILs as well as for the interactions of ILs with molecular solutes. However, such a breakdown into specific and non-specific terms is often arbitrary. For example, many hydrogen bonds are mainly electrostatic.

The electrostatic contribution can be further broken down into terms for interactions between charges, dipole moments, and higher electrostatic moments [Eq. (2)].

$$U_{\text{es}}(r, \Omega) = U_{\text{ion-ion}}(r) + U_{\text{ion-dipole}}(r, \Omega) + U_{\text{dipole-dipole}}(r, \Omega) + U_{\text{ion-quadrupole}}(r, \Omega) \dots \quad (2)$$

In molecular liquids, the dipole–dipole contribution forms the leading term, which, for example, controls the magnitude of the static dielectric constant (relative dielectric permittivity) and therefore the solvation capability. The resulting static dielectric constants for ionic liquids correspond to those of moderately polar molecular solvents^[13] (see also Section 5.1).

The net charge of the particles greatly complicates the understanding of the electrostatic interactions. The charged neighbors around a given particle screen its electrostatic interactions with particles that are located further away. For simple salts, such as NaCl, the screening of the Coulomb forces between the net charges of the ions forms the basis of the understanding of their liquid-phase properties.^[14] However, screening influences all the electrostatic interactions given in Equation (2). Molecular dynamics (MD) simulations show that because of this screening, the dipole–ion and dipole–dipole interactions of a dissolved particle with its neighbors scarcely exceed two solvation shells.^[15] Owing to this localization of the electrostatic interactions it seems necessary to rethink some basic concepts of solvation, these concepts are often based on continuum approximations for the solvent. A first attempt for describing screened interactions in ILs was made by Kobrak.^[15b]

2.3. Salts in the Gaseous Phase

2.3.1. Ion Clusters

Among the differences between ILs and molecular solvents is the practically negligible vapor pressure of ILs, which, in principle, prevents the experimental characterization of the gaseous phase. However, electrospray ionization mass spectrometry (ESI-MS) has allowed ion clusters to be isolated and their stability to be studied.^[16] Such studies have

identified an array of charged and uncharged ion clusters of different sizes.

It is now known that at elevated temperatures the vapor pressure of some ILs is increased sufficiently so that distillation is possible in their thermally stable range, below 500 K,^[17] which opens new perspectives for experiments in the gaseous phase. Very recently, Armstrong et al.^[18] have succeeded in evaporating ionic liquids in high vacuum and analyzing the vapor by mass spectrometric methods. Their results imply that this vapor only comprises neutral ion pairs and that the larger charged and uncharged aggregates found by electrospray mass spectrometry are not present.

2.3.2. The Structure of Ion Pairs

The molecular and electronic structure of an ion pair can be determined by quantum-chemical calculations.^[9,19] The strong electrostatic interactions result in binding energies up to 400 kJ mol^{−1}, which are an order of magnitude larger than those of pairs of uncharged molecules.

Quantum-chemical computations for the [C₄mim]Cl pair^[9,19d] indicate several stable positions of the Cl[−] ion (Figure 1). Conformers with the Cl[−] ion in front of the C2–H

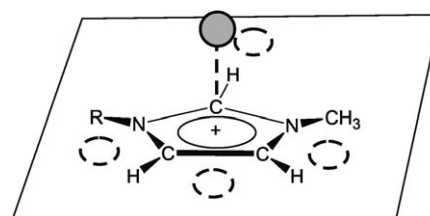


Figure 1. Stable positions of Cl[−] ions relative to the imidazolium cation in the ion pair.^[9,19d] Dashed circles represent in-plane positions, the solid circle a position on top of (or by symmetry, below) carbon C2.

bond and on top of C2 of the imidazolium ring are energetically preferred. In-plane positions near C4–H and C5–H are markedly less stable. The C–H...Cl bridges are essentially ionic.^[9]

The role of the hydrogen bonds between imidazolium ions and larger anions is the subject of controversial debate. In the most stable ion-pair structure of [C₂mim][PF₆]^[19c] the [PF₆][−] ion is placed over the imidazolium ring, with three fluorine atoms forming a triangle with short contacts to C2–H and to the hydrogen atoms of the alkyl groups. Similar out-of-

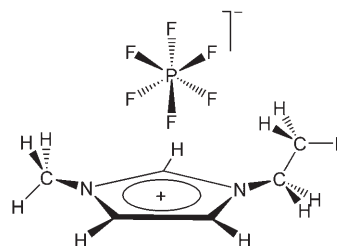


Figure 2. Most stable cation–anion configuration in [C₂mim][PF₆].

plane positions are observed for other large anions, such as $[\text{BF}_4]^-$ and $[\text{Tf}_2\text{N}]^-$. Based on criteria such as bond lengths, bond angles, binding energies, or shifts in vibrational frequencies, the role of C–H \cdots F bonds was assessed to be negligible,^[19c] of minor relevance,^[19e] or essential.^[19b]

2.4. The Structure of the Liquid Phase

2.4.1. Scattering Experiments

In contrast to the long-range structural order in crystals, the phrase “liquid structure” usually refers to local structural features. However, owing to broad distance distributions in ILs, the common X-ray- and neutron-scattering techniques for determining the liquid structure are of limited use. To date, relevant structure determination experiments were only conducted by neutron scattering for three 1,3-dimethylimidazolium salts,^[11,20,21] where selective deuteration of the cation was used to vary the weight of some contributions, and where the symmetry of the cation and the absence of flexible side chains facilitates interpretation.

The most outstanding result of the scattering experiments is the observation of long-range, charge-ordered structures. Figure 3 schematically compares the distribution function

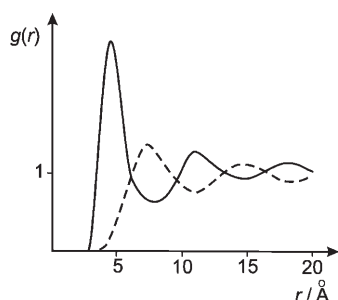


Figure 3. Schematic comparison of the cation–anion pair distribution of the ion centers (solid line) with the like-ion (cation–cation or anion–anion) distributions (dashed line).

$g_{ij}(r)$ for the cation–anion pair with the like-ion (cation–cation or anion–anion) distribution. Oscillations of up to 20 Å (or beyond) indicate several distinct solvation shells, which extend over a much longer range than in molecular liquids. The cation–anion distribution is out of phase with the like-ion distributions, indicating a strongly charge-ordered structure with alternating layers of cations and anions.

Local ion configurations are more difficult to extract from the scattering patterns, and only provide rough information on ion configurations. Figure 4 shows the cation–anion configurations in liquid $[\text{C}_1\text{mim}]\text{Cl}$ derived from the scattering data.^[20] The position of highest probability for the Cl^- ion is in a band around C2–H. There is a lower probability of finding the Cl^- ion in a cylinder around the imidazolium ring. This structure is notably different from the preferred positions of the Cl^- ion in the isolated cation–anion pairs shown in Figure 1. In homologous salts comprising the larger $[\text{PF}_6]^-$ ^[21]

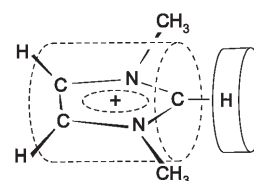


Figure 4. Schematic representation^[9] of the positions of the Cl^- ions in liquid $[\text{C}_1\text{mim}]\text{Cl}$ deduced from scattering data.^[20] The band around C2–H shows positions of high probability. The cylinder around the imidazolium ring shows positions of low probability. The methyl groups exclude some positions within this cylinder.

and $[\text{Tf}_2\text{N}]^-$ ions,^[11] the anions are located above the center of the imidazolium ring.

It is tempting to derive the liquid structure from the crystal structure. Combined X-ray and neutron-scattering experiments of crystalline, glassy, and liquid samples of $[\text{C}_4\text{mim}][\text{PF}_6]$ indeed show that the global structural features of the liquid and solid phases are similar.^[22] This situation does, however, not imply that the local ion configurations are identical. Moreover, different conformers in the liquid and solid phases may result in structures which are not related to one another.^[11]

Many interpretations of the bulk properties of imidazolium salts postulate interactions involving the aromatic π -systems of adjacent cations, such as methyl $\cdots\pi$ interactions, $\pi\cdots\pi$ stacking, or C2–H $\cdots\pi$ interactions in staggered configurations. Although the available scattering experiments for liquid ILs cannot give information about such interactions, but some crystal structures suggest their relevance. For example, in $[\text{C}_1\text{mim}][\text{Tf}_2\text{N}]$ the cations are aligned in layers, enabling $\pi\cdots\pi$ interactions at comparatively short distances.^[12] Yet, the closest cation–cation contacts are van der Waals contacts between methyl groups.^[11,12]

2.4.2. Computer Simulations

In view of the experimental limitations, computational methods are crucial for modeling the liquid structure. Starting with work by Hanke et al.^[23] there has been an ever-increasing number of simulations of the structure, dynamics, and bulk properties of ILs using classical MD methods, which were recently summarized by Hunt.^[24] Many of the studies will be mentioned in later Sections.

The significance of the simulations crucially depends on the quality of the molecular force field used. There are still problems in developing predictive and transferable force fields, this is in part due to the lack experimental data available, such as enthalpies of vaporization, for an accurate parameterization.

Decisive information about the liquid structure should come from ab initio (Car–Parinello-type) quantum-chemical simulations, in which the electronic structure is continually revised during the calculation. To date, such simulations were only conducted for $[\text{C}_1\text{mim}]\text{Cl}$ ^[25] and are limited to a small number of ions and to short simulation times.

In total, simulations have provided results for the structure and bulk properties of many ILs, but most of these

are imidazolium salts. All simulations confirm a pronounced long-range charge order of ILs. Some simulations perform surprisingly well in predicting the structure and bulk properties of ILs, but as discussed in later Sections, there are many unresolved issues, for example, in simulating the phase behavior, viscosity, or electrical conductance.

2.4.3. Hydrogen Bonds in Imidazolium Salts

Controversial experimental and simulation results about local structures mainly concern the existence and strengths of hydrogen bonds between cations and anions. While some authors postulate extended three-dimensional networks of hydrogen bonds,^[26] others point out that there are no clear-cut indications for such bonds.^[27] In part, the controversial interpretations are founded in different criteria used for assessing hydrogen-bonded states, which range from requirements for bond lengths, bond angles, or frequency shifts in spectra to empirical correlations and unsubstantiated arguments.

It is widely agreed that hydrogen-bond formation is favored by the acidic nature of the hydrogen atoms of imidazolium salts and depend largely on the nature of the anion. The complexity of this problem is evident from the structure of [C₁mim]Cl shown in Figure 4. It is tempting to attribute the position of the Cl[−] ion to a C–H⋯Cl bond, but the expected linear C–H⋯Cl configuration is neither confirmed by experiment nor by simulations. Moreover, the C–H⋯Cl configurations in the liquid state (Figure 4) are different from those in isolated pairs (Figure 1). A proper understanding of the phenomenon will probably require extensive quantum-mechanical computations.

The problem of hydrogen bonding between cations and anions is also crucial for understanding the solvation of dissolved particles and the transition states in chemical reactions, because the interaction of a solvating ion with the solute has to compete with the interaction with the counterions. In particular, it seems possible to control the solvation capability of ions by varying the counterions.^[28] In Section 5.4 this behavior will be exemplified by considering the nucleophilicity of halide ions.

2.4.4. Ion Pairs in the Liquid Phase

Another subtle problem concerns the existence of ion pairs (and larger ion clusters) in the liquid state. The existence of ion pairs is apparently supported by the electrical conductance, which does not conform to expectations for fully dissociated systems.^[29] An “ionicity” scale based on conductance data indeed correlates with features derived from computations for isolated pairs.^[30] However, the reduction of the conductance does not necessarily imply the existence long-lived ion pairs (see Section 4.6).^[14]

Some clarification comes from a comparison of results from spectroscopic methods on different time scales. C–H vibrations in FT-IR spectra of [C₂mim][Tf₂N] can be assigned to ion pairs,^[31] but IR spectra map processes on the subpicosecond time scale. Dielectric spectroscopy^[32,33] and NMR spectroscopy^[29] capture processes on the picosecond-to-nano-

second and microsecond-to-millisecond time scale, respectively. On these time scales no signals of ion pairs are detectable, which sets an upper bound for their life time at a few picoseconds.^[32]

Interestingly, in dilute solutions of ILs in CHCl₃ some ion pairs are sufficiently long-lived to provide distinct ion-pair signals in dielectric^[33] and NMR spectroscopy.^[34] However, in dilute solutions a given ion is surrounded by a monotonously decreasing charge density of counterions, the so-called “ion atmosphere”. These conditions differ drastically from the oscillating charge density in neat ILs. Thus, the well-established concept of ion pairs in electrolyte solutions is not transferable to neat ionic liquids.

2.5. Phenomena on Mesoscopic Length Scales

Recently, a mesoscopic organization of ILs has become the subject of debate, which indicates that the morphology of ILs is far more complex than originally expected on the basis of the properties of simple inorganic salts. Nanostructures similar to those observed for concentrated solutions of surfactants were first proposed by Compton et al.,^[35] and were discussed more broadly by Dupont.^[26] Hamaguchi and Ozawa^[10d] have argued that ILs may not be liquids in the conventional sense, but may rather be considered as mesophases.

The most direct evidence for mesoscopic structures comes from the formation of liquid-crystalline phases of salts with long alkyl chains, for example, imidazolium salts with alkyl chains $C_n \geq C_{12}$.^[36] Small-angle X-ray scattering shows that such structural domains survive in the isotropic liquid above the clearing point.^[36c] Crystal structures of salts with shorter alkyl chains also indicate the presence of structural domains.^[37]

Recent work has shown that mesoscopic structures also exist in ILs with shorter alkyl chains, such as imidazolium salts with alkyl chains $C_n \geq C_4$. Several MD simulations, notably that of Canongia Lopes and Padua,^[38] indicate the presence of hydrophilic domains that are formed by the head groups of the cations and anions and of nonpolar domains that are formed by the alkyl groups. With increasing size of the alkyl chains these domains grow and begin to link together.^[38] More recently, X-ray scattering experiments on 1-alkyl-3-methylimidazolium salts ($4 \leq C_n \leq 10$) by Triolo et al.^[39] have given direct experimental evidence for such mesoscopic structures. The scattering patterns show a diffraction peak arising from structural inhomogeneities on the nanometer scale. The size of the inhomogeneities is proportional to the length of the alkyl chains.

In molecular liquids the formation of mesophases is often driven by the shape anisotropy of the molecules and the strong orientation dependence of electrostatic and van der Waals interactions. Dupont^[26] proposed that mesoscopic structures in ILs may be driven by a three-dimensional hydrogen-bonded network. The scattering experiments of Triolo et al.^[39] imply that the head groups of the cations and anions of ILs form a charged matrix, in which the non-polar domains of alkyl chains are embedded.

The consequences that these mesoscopic structures have for the properties of ILs are just beginning to be explored, but many peculiarities of IL behavior may have a natural explanation in terms of heterogeneous structures. For example, some of the peculiarities in the molecular motions of ILs discussed in Section 3.2 are typical for dynamic processes in a heterogeneous environment. Many other phenomena deserve reconsideration. In particular, the current understanding of solvation and its impact on chemical reactions is founded in a more-or-less homogeneous solvent structure. Many models for solvation describe the solvent as a continuum with the properties of the macroscopic phase. For dipolar solvents such continuum descriptions are remarkably successful, but none of these models can be easily transferred to ILs.

Other possible consequences concern diffusion-controlled chemical reactions in ILs. There are many indications, for example from studies of gas solubilities,^[40] that the liquid structure of ILs has large cavities. Channels in mesoscopic domains should favor fast diffusion of small particles, with the solvent acting like a polymer matrix. There are indeed examples for such fast diffusion-controlled chemical reactions.^[41] On the other hand, larger molecules and transition complexes have to break a pronounced solvent structure, which is enthalpically highly unfavorable, but may be compensated by strong entropic effects. Harper and Kobrak^[18] have quoted examples in which the outcome and the rate of reactions have been ascribed to peculiar enthalpic and entropic effects associated with the formation of transition states.

3. Molecular Motions in Ionic Liquids

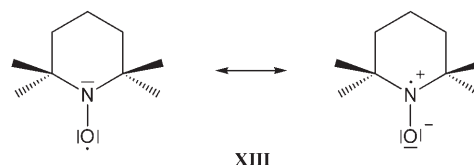
3.1. Experimental Methods for Studying Molecular Motions

Just as important as the knowledge of the structure, is the characterization of the molecular motions of the ions. In low-viscosity ILs the elementary steps of the molecular motions range from femtoseconds to nanoseconds. Table 1 lists some important experimental techniques for probing dynamic processes. Dielectric spectroscopy in the microwave^[32,33,42]

Table 1: Spectroscopic methods for studying molecular motions in ILs.

Method	Dynamical process	Ref.
microwave dielectric spectroscopy	fluctuation of electric dipole moments	[32, 33, 42]
dielectric spectroscopy in the terahertz regime	fluctuation of electric dipole moments	[43]
optical Kerr effect (OKE) spectroscopy	fluctuation of the polarizability anisotropy	[44]
nuclear magnetic relaxation	reorientational dynamics of ions	[45, 46]
quasi-elastic neutron scattering	motions of hydrogen atoms	[47]
electron spin resonance	mobility of spin labels	[48]
time-resolved fluorescence spectroscopy	solvation dynamics	[49]
ultrafast time-resolved fluorescence spectroscopy	fast solvation dynamics	[50]

and far-infrared^[43] regime, optical Kerr effect (OKE) spectroscopy,^[44] nuclear magnetic relaxation (NMR),^[45,46] and quasi-elastic neutron scattering (QENS)^[47] can be used to study molecular motions in neat ionic liquids. Other methods require dissolved probe molecules. An example is electron spin resonance (ESR) which uses spin labels, such as the nitroxide radical TEMPO (**XIII**) and its derivatives (Scheme 4).^[48]



Scheme 4. 2,2,6,6-tetramethylpiperidine-1-oxyl (TEMPO).

In addition, there is particular interest in photophysical methods, such as time-resolved fluorescence spectroscopy, often referred to as “solvation spectroscopy”.^[49,50] This method maps the solvent reorganization around a solvatochromic probe after a sudden change of the probe’s dipole moment through excitation of the probe by a photon. This reorganization is central to the understanding of some solvent-controlled chemical reactions. Scheme 5 compiles some typical solvatochromic probes. A comprehensive discussion of such studies has recently been given by Samanta.^[51]

Whereas the methods mentioned so far use stable molecules as probes, it is also possible to generate transient intermediates by electrochemical methods, pulse radiolysis, or UV-excitation, which can be used to probe the dynamic properties of their environment.^[52] In such studies the effects of solvation dynamics are, however, often masked by chemical processes.

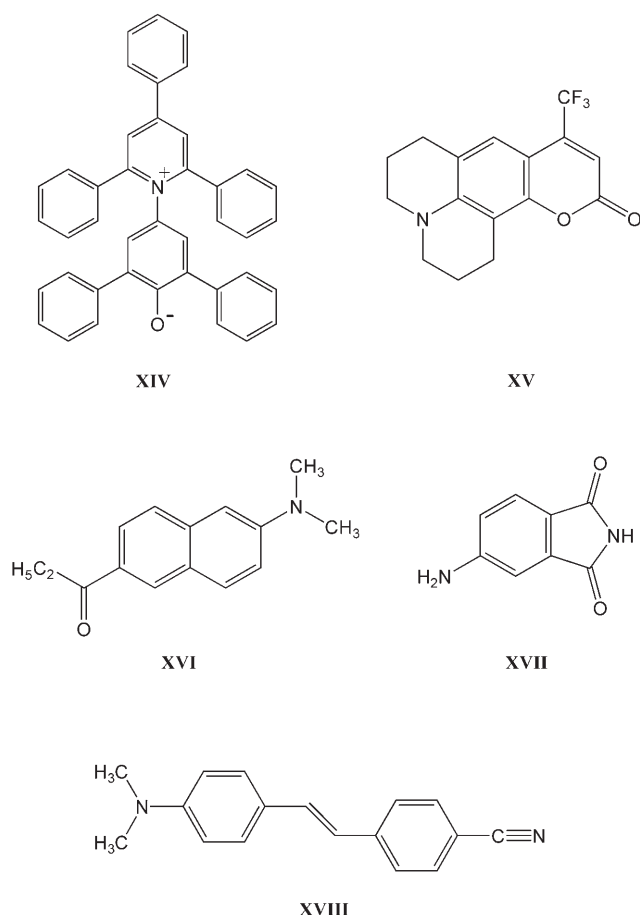
Although the methods listed in Table 1 reflect rotational motions of the ions or have rotational and translational components, experimental information on the mechanisms of purely translational motions is scarce. There is extensive data for self-diffusion coefficients^[29] (see section 4.5) measured by nuclear magnetic resonance spectroscopic methods. The observation time of microseconds to milliseconds of such experiments is, however, too long to provide information on the elementary steps of translational diffusion. Rather, the long-time diffusive behavior given by the Einstein relation [Eq. (3)] is detected where $\langle r^2 \rangle$ is the mean-square displacement of the ions after time t .

$$\langle r^2 \rangle = 6 D_{\text{ion}} t \quad (3)$$

3.2. Molecular Motions in the Liquid Phase

3.2.1. Diffusive Dynamics

The spectrum of molecular motions in low-viscosity ILs extends from “ultrafast” processes on the time scale of femtoseconds to diffusive motions on the nanosecond scale. In supercooled systems the time scale for the diffusive regime



Scheme 5. Solvatochromic probes: **XIV**: betaine-30; **XV**: coumarine-153; **XVI**: prodane; **XVII**: 4-AP (4-aminophthalimide); **XVIII**: DCS (4-dimethylamino-4'-cyanostilbene).

may be displaced by many orders of magnitude and be up to seconds or even longer.^[42]

In simple molecular liquids, diffusive rate processes, such as molecular reorientation, show simple kinetics characterized by exponential relaxation functions of the form given in Equation (4) where τ_D is denoted as “Debye relaxation time”. In contrast, ILs generally show a strongly non-exponential dynamics, as indicated by all the experimental methods listed in Table 1, provided that these methods allow for an adequate time resolution.

$$\Phi(t) = \exp(-t/\tau_D) \quad (4)$$

There is some disagreement on the physical origin of this behavior. In spite of the comparatively low viscosities of the ILs under test, the spectra are reminiscent of the dynamics of glassy materials.^[32, 47, 49b] The latter show a broad distribution of diffusive processes, usually described by the Kohlrausch–Williams–Watts (KWW) stretched exponential function [Eq. (5)]^[53] with stretching exponents $\beta < 1$ where τ_{KWW} is the so-called KWW relaxation time. In glassy systems this non-exponential dynamic is attributed to dynamic processes occurring in spatially heterogeneous states.^[53] The existence of spatial heterogeneities in ILs suggested by small β -values is

consistent with the mesoscopic structures discussed in Section 2.5.

$$\Phi(t) = \exp\{(-t/\tau_{\text{KWW}})^\beta\} \quad (5)$$

In many cases the measured relaxation times provide information about the reorientational motions of ions. Within simple hydrodynamic models, the reorientation times τ_{rot} should be proportional to η/T , where η is the viscosity of the surrounding medium. This dependency has indeed been observed over a wide temperature range.^[44] In contrast to the situation encountered in molecular liquids, there is some evidence^[32, 46] that reorientation times are largely overestimated by hydrodynamic estimates.

3.2.2. Ultrafast Processes

Owing to their key role in the short-time motions in chemical reaction dynamics, large efforts have been made to experimentally characterize ultrafast motions at the subpicosecond time scale. In neat ionic liquids such processes are preferably studied by optical Kerr effect (OKE) spectroscopy, which provides femtosecond time resolution.^[44] In addition the past decade has seen the development of terahertz (THz) spectroscopic methods which extend dielectric spectroscopy to higher frequencies. For ILs terahertz spectroscopy is just beginning to be explored.^[43] OKE and THz spectroscopy provide evidence for intermolecular vibrations and librational motions of ions in the cage formed by their neighbors. Qualitative information on the existence of such processes can also be deduced from high-frequency extrapolations of microwave dielectric spectra.^[32] In dipolar aprotic liquids, pronounced high-frequency processes that contribute to the dielectric spectra are scarce.

3.2.3. Solvation Dynamics

As noted above, solvation spectroscopy provides information on the reorganization of the solvent around a solvatochromic probe (Scheme 5) after excitation of the probe’s dipole moment with a photon. In electron- and proton-transfer reactions, this reorganization controls the rate of the chemical reactions, but in principle, solvent reorganization concerns all reactions involving polar transition states.^[54]

Like the other spectroscopic methods, solvation spectra indicate a broadly distributed diffusive dynamic.^[49] Recently, experiments could be extended to include ultrafast solvation dynamics.^[50] The magnitude of these ultrafast processes is very sensitive to the nature of the cations and anions. Simulations^[55] ascribe the ultrafast processes to jitter motions of the ions in the solvation sphere of the solvatochromic probes.

In total, the spectroscopic data show an unusually broad spectrum of dynamic processes in ILs, which has no analogues in molecular liquids of comparable viscosity. A possible rationale for the broad distribution of dynamics is the heterogeneity of the ILs, which is in accord with the mesoscopic structures of ILs discussed in Section 2.5.

4. Macroscopic Properties of Ionic Liquids

4.1. Melting Behavior

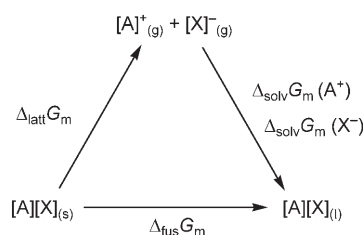
In applications, the utility of an IL largely depends on its melting temperature. The accurate determination of the melting temperature is often difficult because many ILs tend to undergo supercooling and glass formation. Unfortunately, there are no clear-cut features that would enable discrimination between glass formers and salts showing defined melting points. A study of the liquid, amorphous, and polymorphous crystalline states of $[\text{C}_4\text{mim}][\text{PF}_6]$ shows that intrinsic properties, such as conformational equilibria, solid polymorphism, or high viscosities, as well as experimental factors, such as a cooling rates, may be relevant for supercooling behavior.^[22]

An increase in size, anisotropy, and internal flexibility of the ions should lower the melting temperature, T_m , whereas increasing dispersive interactions between alkyl chains, should increase T_m . This expectation is, for example, in agreement with results for homologous imidazolium salts with the $[\text{BF}_4]^-$ ion.^[36] Cations with short alkyl chains ($C_n \leq 3$) form crystalline phases with comparatively high melting temperatures. Salts with alkyl chains of intermediate lengths ($4 \leq C_n < 12$) exhibit a broad liquid range with low melting temperatures, and a pronounced tendency to supercool. Ions with long alkyl chains ($C_n \geq 12$) result in complex phase diagrams, involving liquid-crystalline phases. The effects of anions are more difficult to rationalize, and seem to depend on the electronic structure of the anion and its ability to form hydrogen bonds.

Reliable melting point predictions form a key for the rational design of ILs. From the many attempts to understand the melting behavior, two approaches are selected: First, “quantitative structure–property relationship” (QSPR) methods were used to correlate T_m with “molecular descriptors” derived from quantum-mechanical computations.^[56] QSPR methods are used in many fields of chemistry for data correlation and prediction. However, for calibration, such correlations need melting-point data for the IL family under test. Second, melting temperatures were also derived from thermodynamic cycles. Krossing et al.^[57] have used the Born–Haber–Fajans cycle for calculating the molar Gibbs energy of fusion $\Delta_{\text{fus}}G_m$, and its enthalpic and entropic contributions, $\Delta_{\text{fus}}H_m$, and $\Delta_{\text{fus}}S_m$, given by Equation (6). At the melting temperature $\Delta_{\text{fus}}G_m$ is zero.

$$\Delta_{\text{fus}}G_m = \Delta_{\text{fus}}H_m - T \Delta_{\text{fus}}S_m \quad (6)$$

This rigorous cycle sketched in Scheme 6 relates $\Delta_{\text{fus}}G_m$ to the lattice Gibbs energy for the sublimation of the ions ($\Delta_{\text{latt}}G_m$) and the Gibbs energy of solvation ($\Delta_{\text{solv}}G_m$) for the transfer of ions from the gas phase into the liquid medium. The lattice terms were estimated by a combination of quantum-chemical calculations and thermodynamic approximations. The solvation terms were calculated by the COSMO solvation model,^[58] which assumes a dielectric medium around a gas-phase structure of the ion, and minimizes the energy of the ions within this medium. The Born–Haber–



Scheme 6. Born–Fajans–Haber cycle for calculating the molar Gibbs energy of fusion, $\Delta_{\text{fus}}G_m$, from the lattice Gibbs energy, $\Delta_{\text{latt}}G_m$, and the Gibbs energy of solvation, $\Delta_{\text{solv}}G$. The indexes (s), (l), and (g) refer to the solid, liquid, and gaseous states, respectively.

Fajans cycle model provides basic insights into the processes controlling the melting transition.

4.2. Vapor Pressure and Boiling Temperature

From the applications point of view, the vapor pressures of ILs are negligible, which facilitates their handling as solvents and forms one of the foundations of the “green” nature of ILs. In fact, at room temperature the vapor pressures of ILs are too low to be detected. Eventually, at high temperatures the vapor pressure should become detectable, but in the high-temperature regime the thermal stability of ILs is of concern.

Thermogravimetric analyses of the mass loss upon heating locate the onset of thermal decomposition of many ILs at 700 K. However, for most applications the results of fast thermogravimetric scans under a protective atmosphere are of little relevance. At more realistic conditions and over longer times, ILs will not tolerate such high temperatures. How an IL behaves, varies with the specific cation–anion combination. Thus, $[\text{C}_4\text{mim}][\text{TF}_2\text{N}]$ is thermally stable for 10 h at 473 K, whereas substitution of $[\text{C}_4\text{mim}]^+$ by $[\text{C}_{10}\text{mim}]^+$ and of $[\text{TF}_2\text{N}]^-$ by $[\text{PF}_6]^-$ led to degradation.^[59]

Salts of the $[\text{C}_n\text{mim}][\text{TF}_2\text{N}]$ series should be of sufficient thermal stability to enable studies up to about 600 K. Within a short time three studies have appeared which demonstrate and exploit a measurable vapor pressure of these salts. First, Earle et al.^[17] have shown that some ILs can be evaporated and recondensed below 500 K. Shortly thereafter, Zaitsau et al.^[60] reported the first experimental results for vapor pressures obtained by a Knudsen-type effusion method. The vapor pressures measured by Zaitsau et al.^[60] at about 450–530 K are of the order of 10^{-8} to 10^{-7} bar. Finally, Armstrong et al.^[18] have succeeded in evaporating ILs under high vacuum, and in analyzing the vapor phase by mass spectrometry. Their experiments show that the thermal transfer of ILs into the gaseous phase occurs only via neutral ion pairs. Free ions and larger charged or uncharged ion clusters are not relevant in the gas phase.

Extrapolation of the vapor pressure curves to atmospheric pressure yields hypothetical boiling temperatures of 850–930 K (Table 2).^[60] In the past there have been many attempts to assess the boiling temperatures of ILs. In particular, an analysis of the temperature dependence of the surface tension^[61] based on the Eötvös rule should be mentioned.

Table 2: Molar enthalpy of vaporization, $\Delta_{\text{vap}}H_m^{298}$, and extrapolated normal boiling temperatures, T_b , of ILs at 298 K.

	$\Delta_{\text{vap}}H_m^{298}$ [kJ mol ⁻¹]			T_b [K]
IL	ref. [60]	ref. [64]	ref. [18]	ref. [60]
[C ₂ mim][Tf ₂ N]	135.3	136	134	907
[C ₄ mim][Tf ₂ N]	136.2	155	134	933
[C ₆ mim][Tf ₂ N]	139.8	173	139	885
[C ₈ mim][Tf ₂ N]	150.0	192	149	857

For molecular liquids this rule yields excellent estimates of the critical temperature and normal boiling temperature. For ILs the estimated boiling temperatures are, however, almost 300 K lower than the values deduced from the vapor-pressure curves. The failure may be caused by a pronounced orientational order of the ions at the liquid–vapor interface.^[62,63] The discrepancies illustrate the large difficulties in transcribing rules developed for molecular liquids to ILs.

4.3. Enthalpy of Vaporization and Cohesive Energy Density

The analysis of the vapor-pressure curves^[60] provides molar enthalpies and entropies of vaporization, which can be extrapolated to 298 K. Owing to the strong ionic interactions, the enthalpies of vaporization ($\Delta_{\text{vap}}H_m^{298}$) summarized in Table 2, are by almost an order of magnitude higher than the typical values for molecular liquids. On the other hand, these values are substantially lower than the values of up to 300 kJ mol⁻¹ occasionally quoted in the literature.^[61]

Meanwhile, further experimental data on enthalpies of vaporization have been reported. Table 2 summarizes the available results. Results obtained by a microcalorimetric method by Santos et al.^[64] are markedly larger than those deduced from the vapor-pressure curves. In contrast, results obtained by mass spectrometry by Armstrong et al.^[18] agree excellently with the results of vapor-pressure measurements.

The enthalpy of vaporization ($\Delta_{\text{vap}}H_m$) is an important ingredient in the thermodynamic modeling of equations of state for neat ILs and mixtures, and forms an important measure for molecular interactions in the liquid state. Equation (7) relates $\Delta_{\text{vap}}H_m$ to the cohesive energy density $\Delta_{\text{vap}}U/V_m$ of the liquid phase, where $\Delta_{\text{vap}}U_m$ denotes the molar energy of vaporization, V_m the molar volume of the liquid phase and R the gas constant. The cohesive energy density is often expressed in terms of Hildebrand's solubility parameter δ .^[65]

$$\frac{\Delta_{\text{vap}}U_m}{V_m} = \delta^2 \cong \frac{\Delta_{\text{vap}}H_m - RT}{V_m} \quad (7)$$

For molecular liquids δ correlates with many thermodynamic, kinetic, and spectroscopic properties. Such correlations were transcribed to ILs, deducing $\Delta_{\text{vap}}H_m$ from rate constants of solvent-controlled chemical reactions^[66] and viscosity data.^[67] Both methods provide values of $\Delta_{\text{vap}}H_m$ of the order of 200 kJ mol⁻¹, which are markedly higher than the actual values. Accurate values for the enthalpy of vaporization are crucial for the calibration and validation of

molecular force fields.^[24] However, the remaining discrepancies in Table 2 still prevent the use of enthalpies of vaporization for parameterization.

4.4. Transport Coefficients

4.4.1. Viscosity

The viscosity, η , of an IL is one of the most important materials properties because high viscosities form barriers for many applications and slow down the rate of diffusion-controlled chemical reactions. Many ILs form highly viscous oils. The lowest viscosity observed to date at 298 K ($\eta = 21$ cP for [C₂mim][(CN)₂N]^[68]) is still more than twenty times that of water. In the synthesis of novel ILs, the search for low-viscosity systems plays an essential role.

Figure 5 shows the temperature dependence of the viscosity of two typical salts in a logarithmic plot of η versus

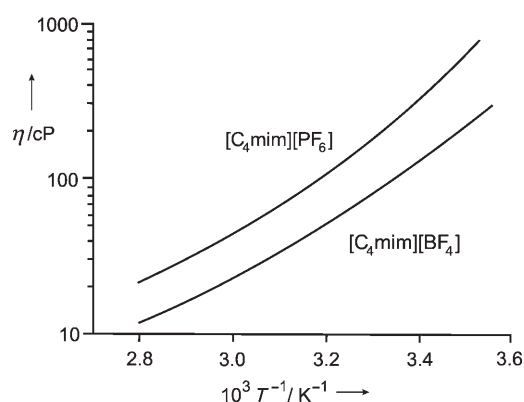


Figure 5: Temperature dependence of the viscosity of [C₄mim][PF₆] and [C₄mim][BF₄].^[69]

the inverse temperature $1/T$. Simple liquids follow the Arrhenius law, according to which this plot yields a straight line. The curvatures in Figure 5 are usually described by the Vogel–Fulcher–Tammann (VFT) equation [Eq. (8)] which comprises three adjustable constants A , B , and T_0 . The equation also applies to other transport properties, such as self-diffusion coefficients, D , of the ions, the electrical conductivity, σ , and some microscopic relaxation times, τ . The plus sign applies to η and τ , the minus sign to D and σ . The temperature T_0 at which the transport coefficients extrapolate to infinity is denoted as the ideal glass-transition temperature. For molecular liquids and ILs T_0 is 30–60 K below the calorimetric glass transition temperature T_g .^[29,70,71] In some models T_0 is given physical significance, for example as the temperature of structural arrest.

$$X = A \exp(\pm B/(T - T_0)) \quad X = \eta, D, \sigma, \tau \quad (8)$$

Deviations from Arrhenius-type behavior provide classification into “fragile glass formers”, for which $\eta(T)$ strongly deviates from Arrhenius behavior and “strong glass formers”, where Arrhenius behavior is obeyed. ILs show fragile or

intermediate behavior.^[70] In models for the glass transition the observed deviations from Arrhenius behavior are consistent with the non-exponential dynamics of ILs, but do not explain why this strongly non-exponential dynamic persists to low viscosities. An analysis of the pressure dependence of the viscosity^[71] reveals notable differences to the typical behavior of molecular liquids.

Simulations of the viscosity are difficult and are just beginning to be explored.^[32c,72] It is therefore interesting to look for simple models for transport processes which may serve for data prediction. Evidence for voids in the liquid structure suggests using free-volume or hole models. In this spirit, Abbott^[73] has applied an old hole model by Fürth. However, for simple molten salts this model was rejected.^[74] It is therefore not clear what the remarkable success of Abbott's model is telling about the molecular mechanisms of transport.

In diffusion-controlled chemical reactions the rate constant should be inversely proportional to the viscosity of the solvent. Because of the high solvent viscosity many chemical reactions are slower in ILs than in molecular solvents, such as water, alcohols, or acetonitrile. In practice, diffusion-controlled processes are usually identified by measuring the temperature dependence of the rate constant because the activation energy of a diffusion-controlled chemical reaction is expected to be equal to the activation energy of the viscosity.^[75]

For diffusion-controlled reactions involving small particles, the experimentally observed rate constants are often distinctly higher than those predicted by simple theories. Clearly, in these cases solute diffusion occurs in channels and voids of the IL structure, and the local friction is insufficiently described by the bulk viscosity. Examples are reactions involving small radicals generated by electrochemical reactions,^[76] or by pulse radiolysis.^[41b] One striking feature is that only the diffusion of small uncharged particles occurs in voids, the diffusion of charged particles of the same size requires a reorganization of the surrounding solvent structure.^[41b,76]

4.4.2. Ion Diffusion

In low-viscosity ILs at 298 K, the self-diffusion coefficients of the cations and anions are of the order of $D \approx 10^{-11} \text{ m}^2 \text{ s}^{-1}$, compared to $D \approx 10^{-9} - 10^{-10} \text{ m}^2 \text{ s}^{-1}$ for simple molecular liquids.^[29] The difference essentially reflects the higher viscosity of ILs.

The diffusion–viscosity relationship is often described by the Stokes–Einstein (SE) equation [Eq. (9) where k_B is the Boltzmann constant] for the diffusion of a sphere of radius r in a hydrodynamic continuum of viscosity η .

$$D = k_B T / \xi \pi \eta r \quad (9)$$

The coupling factor $4 \leq \xi \leq 6$ accounts for the different hydrodynamic boundary conditions at the interface between the diffusing sphere and the viscous medium.

Qualitatively, Equation (9) has been tested for a variety of salts with some success.^[29] However, more recent data for the temperature dependence of the self-diffusion coefficients show physically significant deviations.^[77] Instead of obeying

Equation (9), the data indicate a fractional Stokes–Einstein behavior of the form given by Equation (10) with exponents $m < 1$, for example $m \approx 0.7$.^[77] In glassy dynamics such deviations are well-known, and their extent seems to be closely coupled to the non-exponential relaxation dynamics described by Kohlrausch exponents $\beta < 1$ in Equation (5).^[77]

$$D \propto (T/\eta)^m \quad (10)$$

For molecular liquids, the self-diffusion coefficient is a standard quantity and is often used to validate the quality of the force fields. The usual procedure is to calculate the self-diffusion coefficient from the mean-square displacement of the ions $\langle r(t)^2 \rangle$ at long times t , where $\langle r(t)^2 \rangle$ has a linear dependence on time, so that Equation (3) becomes valid. However, in many simulations, the computed self-diffusion coefficients are strongly underestimated in comparison to experimental data.^[24] This deviation may in part be due to a deficiency in the force fields. However, noting the high viscosity of many ILs, the deficit may also reflect simulation runs that are too short and which do not reach the true asymptotic behavior of $\langle r(t)^2 \rangle$.

4.4.3. Electrical Conductance

Near room temperature, low-viscosity ILs show electrical conductivities, σ , up to $10^{-2} \text{ S cm}^{-1}$, which markedly increase at high temperatures, and compare well with conductivities of some electrolyte solutions used in electrochemistry. In conjunction with an unusually high electrochemical stability of ILs, this conductivity enables innovative electrochemical processes.^[1d,76]

The Nernst–Einstein (NE) equation [Eq. (11)] relates the molar conductance $\Lambda = \sigma/C$ to the self-diffusion coefficients of the ions where C is the molar concentration of the salt and F the Faraday constant.

$$\Lambda_{\text{NE}} = \frac{F^2}{RT} (D_{\text{cation}} + D_{\text{anion}}) \quad (11)$$

This expression would hold rigorously, if the ions were moving independently from one another. A reduction of the conductance relative to the prediction by Equation (11), that is, $\Lambda < \Lambda_{\text{NE}}$, can be rationalized by a coupled motion of cations and anions in electrically neutral configurations, in which the ions contribute to diffusion, but not to the electrical conductance. Values of $\Lambda/\Lambda_{\text{NE}} < 1$ were indeed observed a long time ago for molten alkali halides^[14] and in 1990 similar results were reported for some tetraalkylammonium tetraalkylborides.^[78] Meanwhile this reduction in electrical conductance is well established for many ILs.^[29] Often, about half of the ions apparently do not contribute to the electrical conductance.

In view of the current debate about the existence of ion pairs in the liquid phase, a proper understanding of the deviations from Equation (11) is mandatory. Because the reduction in conductance reflects collective motions of ions in aggregates, MD simulations are difficult. Although such simulations were reported for NaCl as early as 1975,^[14] they

are just beginning to be explored for ILs.^[79] The results available to date show that the reduction in conductance does not require the existence of long-lived ion pairs. Rather, it results from short-lived neutral configurations of ions. This situation confirms the observations regarding the life time of ion pairs discussed in Section 2.4.

5. Solvent Properties of Ionic Liquids

5.1. Static Dielectric Constant

When selecting the solvent for a given application, the polarity often forms the most important criterion because it describes the global solvation capability of the solvent. The solvation capability reflects a complex interplay of molecular interactions. Because different experimental methods highlight different facets of these interactions, many method-dependent polarity scales exist, ranging from one-parameter representations to multiparameter approaches based on “linear free energy relationships”.

For molecular liquids the relative dielectric permittivity, ϵ_s , usually denoted as the static dielectric constant, is a key quantity for describing the solvent polarity. Many approaches for describing solvation describe the solvent as a dielectric continuum with the dielectric constant of the bulk liquid ϵ_s . Because of the electrical conductance of ILs, conventional methods for measuring ϵ_s fail. The dielectric constant of ILs was therefore widely believed to be immeasurable. However, it is long known that dielectric constants of electrolyte solutions can be determined by measuring the frequency-dependent dielectric permittivity and subsequent extrapolation to zero frequency. For low-viscosity systems this frequency dependence falls into the frequency range of about 100 MHz to 20 GHz,^[32,33] which is covered by microwave spectroscopy. In the case of ILs, this method was first applied to ethylammonium nitrate.^[80]

Table 3 summarizes some dielectric constants of imidazolium salts.^[13b] The data classify ILs as moderately polar

Table 3: Dielectric constants of some imidazolium salts at 298.15 K.^[13b]

Cation	[BF ₄] [−]	[PF ₆] [−]	[Tf ₂ N] [−]	[TfO] [−]	[EtOSO ₃] [−]
[C ₂ mim] ⁺	12.9		12.3	15.1	27.9
[C ₃ mim] ⁺			11.6		
[C ₄ mim] ⁺	11.7	11.4	11.6	13.2	
[C ₅ mim] ⁺			11.4		

solvents, in particular, if the dipolar cations are paired with anions of vanishing or low dipole moment, such as [BF₄][−], [PF₆][−], or [Tf₂N][−]. For a given anion the values are remarkably insensitive to the nature of the cation. In general, ϵ_s is lower than values derived from other measures of assessing the polarity.^[13] Anions with high dipole moments, for example alkylsulfates, may cause a marked increase of ϵ_s .

Simulations of dielectric behavior are exceedingly difficult because dielectric phenomena reflect a collective prop-

erty of the total assembly of particles rather than a single-particle property. The only simulation available to date shows that the dielectric polarization results mainly from the orientational polarization of dipolar ions.^[27] Thus, the mechanism responsible for the dielectric behavior does not seem to be notably different from that encountered in molecular liquids. The comparatively low values of ϵ_s just reflect the trivial effect that the large molecular volumes of the ions give rise to low dipole densities. Even at low dipole density, high dielectric constants may, however, be achieved if the dipoles are aligned parallel to each other. The simulations show that the charge-ordering in ILs does not result in such “super-polar” structures.

5.2. Spectroscopic Methods for Determining the Solvent Polarity

Table 4 summarizes some representative examples of studies of the solvent polarity of ILs. These comprise spectroscopic methods, liquid–liquid and liquid–gas distribution equilibria, and methods which map the polarity by means of solvent effects upon chemical reactions.

Table 4: Some methods for characterizing the solvent polarity of ILs.

Method	Ref.
dielectric constant	[13]
UV/Vis and fluorescence spectra of solvatochromic dyes	[82–86]
IR and Raman spectra of dissolved molecules	[87]
electron spin resonance of spin labels	[48]
combined analysis of spectra of several solvatochromic dyes	[28, 89]
liquid–liquid distribution coefficients	[90]
inverse gas chromatography	[91]
solvent effects upon chemical reactions	[28, 96]

Most studies of the solvent polarity of ILs have relied on spectroscopic techniques. The most prominent polarity scale is based on the solvatochromic shift of the low-frequency band in the Vis absorption spectrum of Reichardt’s zwitterionic dye betaine-30 (**XIV**; Scheme 5).^[81] This shift can be expressed in terms of a normalized polarity parameter, E_T^N , which is set at one for water and zero for tetramethylsilane. E_T^N values for ILs have been compiled by Reichardt.^[82] A recent theoretical study of the origin of these shifts was presented by Cavivato et al.^[83]

Selected E_T^N values in Table 5 along with results obtained with other dyes^[84] attribute ILs with a polarity similar to that of methanol, acetonitrile, or DMSO, which is markedly higher than that assessed from dielectric constants. Quantum-chemical computations^[83] and simulations^[15a] show that the negatively charged phenolate oxygen of the zwitterion **XIV** forms hydrogen bonds to cations, whereas the delocalization of the positive charge over the aromatic rings reduces interactions with anions. The fluorescence bands of polycyclic aromatic hydrocarbons, such as the π – π^* emission of pyrene,^[85] mimic the dielectric behavior more directly because the IL–dye interaction is essentially electrostatic.

Table 5: Normalized solvatochromic shift $E_T^{N[82,83]}$ and polarity parameters $\pi^*[28]$ for ILs compared to values for representative molecular liquids. Values in italics are fixed by convention.

	Ionic liquids				Molecular liquids		
	ϵ_s	E_T^N	π^*		ϵ_s	E_T^N	π^*
[C ₂ mim][BF ₄]	12.9	0.710		water	78.4	1	1.09
[C ₂ mim][Tf ₂ N]	12.3	0.676		DMSO	46.7	0.444	1
[C ₄ mim][BF ₄]	11.7	0.673	1.047	ethanol	24.3	0.654	0.54
[C ₄ mim][PF ₆]	11.4	0.667	1.032	dichloromethane	9.1	0.309	
[C ₄ mim][Tf ₂ N]	11.6	0.642	0.984	cyclohexane	2.0	0.006	0.73
[C ₄ mim][TfO]	13.2	0.667	1.006	TMS	1.92	0	0

A detailed analysis of the spectral shift is available for coumarine-153 (**XVI**), in which both absorption and emission can be observed in fluorescence experiments.^[86] The Stokes shift determined in these experiments provides information about the Gibbs energy of solvation, $\Delta_{\text{solv}}G$, and the solvent reorganization energy, λ , resulting from the electronic excitation ($S_0 \rightarrow S_1$) of the dye. In dipolar solvents these energetics are well described by dielectric continuum approaches, which, among other things, predict a proportionality of $\Delta_{\text{solv}}G$ to the so-called reaction field factor $f = (\epsilon_s - 1)/(\epsilon_s + 2)$, thus providing an relationship to the dielectric constant ϵ_s of the solvent. An analysis of about 20 ILs by Jin et al.^[86] shows that this well-established correlation for dipolar solvents cannot be transcribed to ILs.

In addition to solvatochromic shifts, a multitude of other spectroscopic parameters can be used to probe the polarity of ILs. Typical examples are IR and Raman modes of dissolved molecules^[87] or the ESR signal of spin labels, such as the nitroxide radical TEMPO (**XIII**) and its derivatives (Scheme 4),^[48] in which the ¹⁴N hyperfine coupling constant can serve as a polarity probe.

The popular classification of molecular liquids into dipolar aprotic and polar protic solvents suggests breaking down the polarity into components. A well-known approach by Kamlet, Abboud, and Taft^[88] uses a combination of different dyes to break the solvatochromic shift down into contributions of different interactions. Crowhurst et al.^[28] have applied this method to ILs. Oehlke et al.^[89] have optimized the dyes to specifically map the various contributions.

In the present context, the dipolarity parameter π^* listed in Table 5^[28] is of special interest because this parameter maps electrostatic interactions that are also captured by the dielectric constant. π^* is normalized to zero for cyclohexane and to one for DMSO. The values obtained for ILs are distinctly higher than those for dipolar solvents, which contradicts the behavior of the dielectric constant. Because π^* reflects the ability to induce a dipole moment in the probe molecule, π^* should, among other things, reflect interactions of the probe molecules with the net charges of the ions. This contribution, which is not encountered in molecular liquids, may rationalize the consistently high π^* values for ILs. However, this additional mechanism also implies that concepts for rationalizing the polarity of molecular liquids are not easily transferable to ILs.

5.3. Distribution Equilibria

Another approach attempts to assess the polarity by liquid–liquid^[90] or liquid–gas^[91] partitioning. In particular, gas chromatography with ILs as the stationary phase (inverse GC) has enabled their interactions with molecular solvents to be studied.^[91] A model by Abraham^[92] was used to assess different contributions to the polarity of ILs.^[91] Compared to the dielectric constant, the resulting dipolarity parameters^[91] are unexpectedly high.

The solute–IL interaction observed by GC can be quantitatively expressed in terms of the limiting activity coefficient, γ_i^∞ , of the solute i at infinite dilution (index “ ∞ ”) in the IL.^[93] γ_i^∞ is of key interest in separation processes, such as liquid extraction or extractive distillation, because the selectivity $S_{ij}^\infty = \gamma_i^\infty/\gamma_j^\infty$ is a measure for the capability of a solvent for separating two solutes i and j . An outstanding feature of ILs is the high selectivity for separating aromatic and aliphatic compounds, exemplified in Table 6 for *n*-hexane–benzene separation.^[94] This selectivity opens alternatives to conventional methods. The remarkable difference in selectivity is founded in interactions of the ionic charge with the quadrupole moment of aromatic species [cf. Eq. (2)], which is not present for aliphatic solutes.^[95]

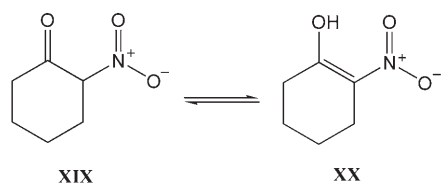
Table 6: Comparison of the selectivities $S_{ij}^\infty = \gamma_i^\infty/\gamma_j^\infty$ for *n*-hexane–benzene separation of ILs with the selectivities of conventionally used molecular solvents.^[94]

Molecular solvents	S_{ij}^∞	Ionic liquids	S_{ij}^∞
sulfolane	30.5	[C ₂ mim][C ₂ OSO ₃]	41.4
dimethylsulfoxide	22.7	[C ₂ mim][Tf ₂ N]	24.4
1-methylpyrrolidine-2-on	12.5	[C ₆ mim][BF ₄]	23.1
		[C ₄ mim][Tf ₂ N]	16.7

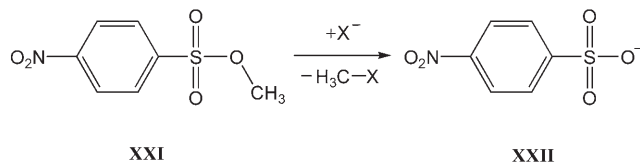
5.4. The Role of Solvent Polarity in Chemical Reactions

The polarity of the solvent can affect chemical reactions in solution, opening the possibility to steer such reactions by careful choice of the solvent. Correspondingly, the influence of solvent effects on chemical reactions has also been used to probe the polarity of ILs.^[11,28,96] For example, Angellini et al.^[96a] have used the keto–enol tautomerism of 2-nitrocyclohexanone (Scheme 7) in conjunction with the solvatochromic shift of the enol form (**XX**) as a measure for the solvent polarity. The effective dielectric constants estimated from these experiments imply a more polar local environment than estimated from the bulk dielectric constant.

Studies of the nucleophilicity of the anions of ILs may be exemplified by considering the S_N2 reaction of methyl-4-nitrobenzenesulfonate (**XXI**) with halide ions to form 4-nitrobenzenesulfonate (**XXII**) and halomethane (Scheme 8).^[97] In ILs the nucleophilicity of the I[−] ion in Scheme (8) was found to depend little on the nature of the cation, while that of the Cl[−] ion showed a strong cation



Scheme 7. Keto–enol tautomerism of 2-nitrocyclohexanone.



Scheme 8. S_N2 reaction of methyl-4-nitrobenzenesulfonate (XXI) with halide ions to form the 4-nitrobenzenesulfonate anion (XXII) and halomethane.

dependence. Clearly, the formation of the activated complex requires the separation of the anion from the surrounding cations, which is hampered by strong cation–anion interactions. In imidazolium chlorides, these interactions are distinctly stronger than in imidazolium iodides. In tetraalkylammonium salts, where hydrogen bonds are unlikely, the nucleophilicity of anions is strongly enhanced.^[97c] The possibility to steer the nucleophilicity, or more generally, the solvent polarity, by variation of the counterion, reflects a unique feature of ILs. Theoretical models for nucleophilic substitutions do not account for such effects.

5.5. Gas Solubility in Ionic Liquids

Interactions between ILs and simple molecular substances are reflected by, among others, the solubility of gases. Since Brennecke and co-workers reported very high solubilities of CO_2 in ILs,^[40] there have been many studies of gas solubilities in ILs. Heintz^[93] has summarized many relevant investigations, and there is still much activity.^[98]

Figure 6 shows the solubility isotherm of CO_2 in $[\text{C}_6\text{mim}][\text{BF}_4]$ at 330 K as a function of pressure;^[99] x_2 is the mole fraction of CO_2 in the liquid phase. High pressures impose a very high solubility. The solubility isotherm behaves quite atypically. In molecular solvents the solubility initially remains low at low pressures, and then increases rapidly, implying an opposite curvature to that displayed in Figure 6.

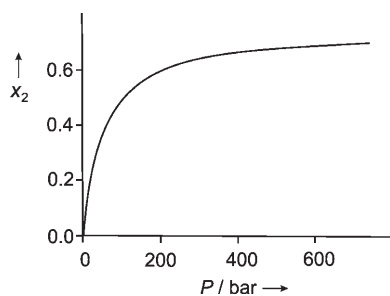


Figure 6. Solubility of CO_2 in $[\text{C}_6\text{mim}][\text{BF}_4]$ at 330 K as a function of pressure.^[99]

Chemists and engineers have an arsenal of empirical or semi-empirical approaches for correlating and predicting gas solubilities. Notably, the curve in Figure 6 resembles an adsorption isotherm, suggesting a simple description in terms of gas adsorption at some kind of “inner surface” of the IL.^[93] Such a simple model also agrees with the observation that dissolved CO_2 does not substantially change the volume of the liquid phase. The picture resulting from simulations^[100] suggests that CO_2 can be intercalated in cavities of the IL structure without markedly affecting it. Thereby, CO_2 preferably optimizes its interactions with anions, with the electrical quadrupole moment of CO_2 playing a crucial role. In fact, anion variation affects the solubility of CO_2 much more strongly than cation variation.^[101]

The solubilities of other gases can also be understood in terms of ion–solute interactions. Simple gases undergo weak dispersive interactions with the ions, and hence, the solubility reflects the molecular polarizability of the solute, giving the series $\text{H}_2 < \text{O}_2 < \text{CH}_4 < \text{C}_2\text{H}_6$. Higher solubilities are achieved for gases such as ethene or CO_2 which have an electric quadrupole moment. Not surprisingly, polar gases, such as SO_2 ^[98c] and water vapor,^[102] show very high solubilities.

5.6. Mixing Behavior with Molecular Solvents

There are numerous reports about the miscibility of ILs with organic solvents, but accurate studies of liquid–liquid coexistence curves are scarce. In general, the widths of the miscibility gaps narrow at high temperatures and the liquid–liquid two-phase regimes terminate at an upper critical solution temperature. An inverse behavior, that is, immiscibility at high temperatures, was recently observed for chloroform.^[103] All the miscibility gaps are highly asymmetrical. The IL can dissolve an appreciable amount of the molecular solvent, whereas the solubility of the IL in the molecular solvent is low.

If the molecular components of the mixtures are arranged with increasing polarity, the mutual solubility of molecular solvents with ILs is lost at either end of the scale. ILs are immiscible with nonpolar hydrocarbons, but hydrophobic ILs are also immiscible with polar solvents of high cohesive energy density, such as water. For solutions of tetraalkylammonium salts this behavior was already observed some time ago.^[104]

The phase behavior can be understood by a semi-empirical theory, which combines the exact Debye–Hückel electrolyte theory for highly dilute solutions with semi-empirical terms for specific ion–solvent interactions.^[104] Model calculations by Schröder and co-workers based on these ideas^[105] show that in mixtures of ILs with molecular solvents of low polarity, liquid–liquid phase separation is driven by Coulombic forces, because free ions and ion clusters do not mix with nonpolar solvents. On the other hand, solvents of high cohesive energy density, such as water or polyalcohols, result in “solvophobic” immiscibility, which is driven by forces similar to those encountered in phase separations of aqueous solutions of hydrophobic solvents.^[104,106]

Many studies apply empirical or semi-empirical approaches developed for molecular systems, such as the COSMO model, to describe these phase equilibria. Without suitable modification, such approaches ignore the rigorous physical limiting conditions given by the Debye–Hückel theory for dilute salt solutions, so that the results, particularly for dilute solutions, are physically meaningless.

Finally, mixtures of hydrophobic ILs with water deserve some comments. ILs with strongly hydrophobic cations or anions are immiscible with water. However, complete immiscibility never exist, and salts can absorb marked amounts of water, often as unwanted impurities. Although for aqueous solutions of imidazolium salts little data exists for plotting coexistence curves, studies of tetraalkylammonium salts reveal closed immiscibility loops with both an upper and a lower consolute point.^[104,106] It is still open, whether other hydrophobic families of salts also show closed-loop behavior.

Whereas in homologous series of cations, the miscibility is rather simply correlated with their hydrophobicity, the effects of anions are less transparent. Systematic studies of tetraalkylammonium salts^[104] have shown that miscibility obeys the so-called Hofmeister series $F^- > Cl^- > Br^- > [NO_3]^- > I^- > [ClO_4]^-$. Originally, this series was deduced from salt effects on the thermal stability of proteins, but it also describes salt effects in simpler systems. There is no doubt that the anion effects on the miscibility of ILs with water will follow similar rules. Pronounced anion–water interactions are shown by spectroscopic studies, simulations, and quantum-chemical computations for anion–water clusters.^[87a,100d,107] As long as water is the minor component of the mixture, the water molecules are not able to form hydrogen-bonded networks, instead they are bound in anion...HOH...anion complexes.

6. Conclusions

ILs display Coulombic interactions between the net charges of the ions as well as interactions between complex chemical groups. Modern experimental and theoretical methods provide an increasing insight into the interplay of these different contributions.

The results of scattering experiments in conjunction with simulations have revealed important information on the liquid structure of ILs. The most spectacular observation concerns the existence of a nanostructure. How this microheterogeneous structure affects the macroscopic properties, solvation, and chemical reactions in ILs remains to be explored.

Just as important as the knowledge of the liquid structure is the characterization of molecular motions. Practically all experimental methods indicate broadly distributed dynamics of the ions, which is untypical for molecular solvents of similar viscosity. It is suggestive to attribute these unusual features to a microheterogeneous environment of the moving particles. A proper understanding of these motions should make it possible to understand and to steer solvent-controlled chemical reactions in ILs.

Recently, sophisticated experimental techniques have enabled the determination of properties of ILs, such as the

vapor pressure, enthalpy of vaporization, or dielectric constant, which for a long time were believed to be immeasurable. In the past, the lack of information on these properties has led to many estimates and speculations; many of these speculations have now been shown to be largely in error. Clearly, some well-established rules and correlations for the behavior of molecular liquids cannot be transferred to ILs in a straightforward way. The peculiar features of molecular interactions between charged particles also requires a careful rethinking of the basic concepts of solvation.

Finally, it should be noted that the present knowledge about the molecular properties of ILs mainly concerns imidazolium salts. Owing to the peculiarities of the electronic properties of imidazolium cations, it may be questioned, whether the molecular picture developed for them to date reflects generic features of ILs. The available results for other salt families, in part, outline a highly variable behavior. It is just this high variability, which will open fascinating possibilities to alter the solvent and materials properties of ILs of over wide ranges.

The Deutschen Forschungsgemeinschaft is thanked for financial support within the priority program SPP 1191 (Ionic Liquids).

Received: December 7, 2006

Revised: June 14, 2007

Published online: November 12, 2007

- [1] a) *Ionic Liquids in Synthesis* (Eds.: P. Wasserscheid, T. Welton), Wiley-VCH, Weinheim, **2003**; b) P. Wasserscheid, A. Keim, *Angew. Chem.* **2000**, *112*, 3926; *Angew. Chem. Int. Ed.* **2000**, *39*, 3772; c) S. A. Forsyth, J. M. Pringle, D. R. MacFarlane, *Aust. J. Chem.* **2004**, *57*, 113; d) F. Endres, S. Zein El Abedin, *Phys. Chem. Chem. Phys.* **2006**, *8*, 2101; e) J. Dupont, P. A. Z. Suarez, *Phys. Chem. Chem. Phys.* **2006**, *8*, 2441; f) C. Chiappe, D. Pieraccini, *J. Phys. Org. Chem.* **2005**, *18*, 275; g) J. B. Harper, M. N. Kobra, *Mini-Rev. Org. Chem.* **2006**, *3*, 253.
- [2] P. Walden, *Bull. Acad. Imp. Sci. St.-Petersbourg* **1914**, *8*, 405; P. Walden, *Chem. Zentralbl.* **1914**/I, 1800.
- [3] F. H. Hurley, T. P. Wier, Jr., *J. Electrochem. Soc.* **1951**, *98*, 207.
- [4] a) T. Welton, *Chem. Rev.* **1999**, *99*, 2071; b) R. L. Hussey in *Chemistry of Nonaqueous Solutions* (Eds.: G. Mamantov, A. I. Popov), VCH, Weinheim, **1994**, pp. 227–276; c) R. T. Carlin, J. S. Wilkes in *Chemistry of Nonaqueous Solutions* (Eds.: G. Mamantov, A. I. Popov), VCH, Weinheim, **1994**, pp. 277–306.
- [5] a) J. S. Wilkes, M. J. Zaworotko, *J. Chem. Soc. Chem. Commun.* **1992**, 695; b) E. I. Cooper, E. J. M. O'Sullivan, *Proc. Electrochem. Soc.* **1992**, *16*, 386 (8th Int. Symp. Molten Salts, **1992**); c) Y. Chauvin, L. Musmann, H. Olivier, *Angew. Chem.* **1995**, *107*, 2941; *Angew. Chem. Int. Ed.* **1995**, *34*, 2698; d) P. A. Z. Suarez, J. E. L. Dullius, S. Einloft, R. F. De Souza, J. Dupont, *Polyhedron* **1996**, *15*, 1217; e) P. Bonhôte, A.-P. Dias, N. Papageorgiou, K. Kalyanasundaram, M. Grätzel, *Inorg. Chem.* **1996**, *35*, 1168.
- [6] A. Arce, M. J. Earle, S. P. Katdare, H. Rodriguez, K. R. Seddon, *Chem. Commun.* **2006**, 2548.
- [7] G. S. Fonseca, A. P. Umpierre, P. F. P. Fichtner, S. R. Teixeira, J. Dupont, *Chem. Eur. J.* **2003**, *9*, 3263, and references therein.
- [8] J. M. Pringle, J. Golding, K. Baranyai, C. M. Forsyth, B. B. Deacon, J. L. Scott, D. R. MacFarlane, *New J. Chem.* **2003**, *27*, 1504.

- [52] a) J. F. Wishart, S. I. Lall-Ramnarian, R. Raju, A. Scumpia, S. Bellevue, R. Ragbir, R. Engel, *Radiat. Phys. Chem.* **2005**, 72, 99, and references therein; b) H. Brands, N. Chandrasekhar, A.-N. Unterreiner, *J. Phys. Chem. B* **2007**, 111, 4830.
- [53] M. D. Ediger, *Annu. Rev. Phys. Chem.* **2000**, 51, 99.
- [54] H. Sumi, R. A. Marcus, *J. Chem. Phys.* **1986**, 84, 4272.
- [55] a) M. N. Kobrak, *J. Chem. Phys.* **2006**, 125, 064502; b) M. N. Kobrak, V. Znamenskiy, *Chem. Phys. Lett.* **2004**, 395, 127; c) Y. Shim, M. Y. Choi, H. J. Kim, *J. Chem. Phys.* **2005**, 122, 044511.
- [56] R. Katritzky, R. Jain, R. A. Lomaka, R. Petrukhin, M. Karelson, A. E. Visser, R. D. Rogers, *J. Chem. Inf. Comput. Sci.* **2002**, 42, 225, and references therein.
- [57] I. Krossing, J. M. Slaterry, C. Daguenet, P. J. Dyson, A. Oleinikova, H. Weingärtner, *J. Am. Chem. Soc.* **2006**, 128, 13427.
- [58] A. Klamt, G. Schürmann, *J. Chem. Soc. Perkin Trans. 2* **1993**, 799.
- [59] M. Kosmulski, J. Gustafson, J. B. Rosenholm, *Thermochim. Acta* **2004**, 412, 47.
- [60] D. H. Zaitsau, G. J. Kabo, A. A. Strechman, Y. U. Paulechka, A. Tschersich, S. P. Verevkin, A. Heintz, *J. Phys. Chem. A* **2006**, 110, 7303.
- [61] L. P. N. Rebelo, J. N. Canongia Lopes, J. M. S. S. Esperança, E. Filipe, *J. Phys. Chem.* **2005**, 109, 6040.
- [62] a) V. Halka, R. Tsekov, W. Freyland, *Phys. Chem. Chem. Phys.* **2005**, 7, 2038; b) S. Rivera-Rubero, S. Baldelli, *J. Phys. Chem. B* **2006**, 110, 4756.
- [63] T. Yan, S. Li, W. Jiang, X. Gao, B. Xiang, G. A. Voth, *J. Phys. Chem. B* **2006**, 110, 1800, and references therein.
- [64] L. M. N. B. Santos, J. N. Canongia Lopes, J. A. P. Coutinho, J. M. S. S. Esperança, L. R. Gomes, I. M. Marrucho, L. P. N. Rebelo, *J. Am. Chem. Soc.* **2007**, 129, 284.
- [65] See, for example: J. H. Hildebrand, J. M. Prausnitz, R. L. Scott, *Regular and Related Solutions*, Van Nostrand-Reinhold, New York, **1970**.
- [66] K. Swiderski, A. E. McLean, C. M. Gordon, D. H. Vaughn, *Chem. Commun.* **2004**, 2178.
- [67] S. H. Lee, S. B. Lee, *Chem. Commun.* **2005**, 3469.
- [68] D. R. MacFarlane, J. Golding, S. Forsyth, G. B. Deacon, *Chem. Commun.* **2001**, 1430.
- [69] K. R. Seddon, A. Stark, M.-J. Torres, *Am. Chem. Soc. Symp. Ser.* **2002**, 7, 43.
- [70] W. Xu, E. I. Cooper, C. A. Angell, *J. Phys. Chem. B* **2003**, 107, 6170.
- [71] a) K. R. Harris, L. A. Woolf, M. Kanakubo, *J. Chem. Eng. Data* **2005**, 50, 1777; b) K. R. Harris, M. Kanakubo, L. A. Woolf, *J. Chem. Eng. Data* **2007**, 52, 1080.
- [72] Z. Hu, C. J. Margulis, *J. Phys. Chem. B* **2007**, 111, 4705, and references therein.
- [73] P. Abbott, *ChemPhysChem* **2004**, 5, 1242.
- [74] See, for example: S. J. Yosim, H. Reiss, *Annu. Rev. Phys. Chem.* **1968**, 19, 59.
- [75] a) C. M. Gordon, A. J. McLean, *Chem. Commun.* **2000**, 1395; b) A. J. McLean, M. J. Muldoon, C. M. Gordon, I. R. Dunkin, *Chem. Commun.* **2002**, 1880.
- [76] D. S. Sylvester, R. G. Compton, *Z. Phys. Chem.* **2006**, 220, 1247.
- [77] a) S. H. Chung, R. Lopado, S. G. Greenbaum, H. Shiroka, E. W. Castner, Jr., J. F. Wishard, *J. Phys. Chem. B* **2007**, 111, 4885; b) K. L. Ngai, *J. Phys. Chem. B* **2006**, 110, 26214.
- [78] N. Weiden, B. Wittekopf, K. G. Weil, *Ber. Bunsen-Ges.* **1990**, 94, 353.
- [79] M. G. Del Popolo, G. A. Voth, *J. Phys. Chem. B* **2004**, 108, 1744.
- [80] H. Weingärtner, A. Knocks, W. Schrader, U. Kaatz, *J. Phys. Chem. A* **2001**, 105, 8646.
- [81] See, for example: C. Reichardt, *Solvents and Solvent Effects in Chemistry*, Wiley-VCH, Weinheim, **2003**.
- [82] C. Reichardt, *Green Chem.* **2005**, 7, 339.
- [83] M. Cavivato, B. Mennucci, J. Tomasi, *Mol. Phys.* **2006**, 104, 875.
- [84] K. A. Fletcher, I. A. Storey, A. E. Hendricks, S. Pandey, *Green Chem.* **2001**, 3, 210.
- [85] S. N. Baker, G. A. Baker, M. A. Kane, F. V. Bright, *J. Phys. Chem. B* **2001**, 105, 9663.
- [86] H. Jin, G. A. Baker, S. Arzhantsev, J. Dong, M. Maroncelli, *J. Phys. Chem. B* **2007**, 111, 7291.
- [87] a) T. Köddermann, C. Wertz, A. Heintz, R. Ludwig, *Angew. Chem.* **2006**, 118, 3780; *Angew. Chem. Int. Ed.* **2006**, 45, 3697; b) G. Tao, M. Zhou, X. Wang, Z. Chen, D. G. Evans, Y. Kou, *Aust. J. Chem.* **2005**, 58, 327; c) T. Fujisawa, M. Fukuda, M. Terazima, Y. Kimura, *J. Phys. Chem. A* **2006**, 110, 6164.
- [88] M. J. Kamlet, J. L. M. Abboud, R. W. Taft, *Prog. Phys. Org. Chem.* **1981**, 13, 485.
- [89] A. Oehlke, K. Hofmann, S. Spange, *New J. Chem.* **2006**, 30, 533.
- [90] M. H. Abraham, A. M. Zissimos, J. G. Huddleston, H. D. Willauer, R. D. Rogers, *Ind. Eng. Chem. Res.* **2003**, 42, 413.
- [91] J. L. Anderson, J. Ding, T. Welton, D. W. Armstrong, *J. Am. Chem. Soc.* **2002**, 124, 14247.
- [92] M. H. Abraham, *Chem. Soc. Rev.* **1993**, 22, 73; and references therein.
- [93] A. Heintz, *J. Chem. Thermodyn.* **2005**, 37, 525; and references therein.
- [94] T. M. Letcher, A. Marciniak, M. Marciniak, U. Domanska, *J. Chem. Eng. Data* **2005**, 50, 1294.
- [95] C. G. Hanke, H. Johansson, J. B. Harper, R. M. Lynden-Bell, *Mol. Phys.* **2004**, 102, 85.
- [96] a) G. Angelini, C. Chiappe, P. D. M. A. Fontana, F. Gasparrini, D. Pieraccini, M. Perini, G. Siani, *J. Org. Chem.* **2005**, 70, 8193; b) K. Baba, H. Ono, E. Itoh, S. Itoh, K. Noda, T. Usui, K. Ishihara, M. Inamo, H. D. Takagi, T. Asano, *Chem. Eur. J.* **2006**, 12, 5328.
- [97] a) N. L. Lancaster, T. Welton, *J. Org. Chem.* **2004**, 69, 5986; b) N. L. Lancaster, *J. Chem. Res.* **2005**, 413; c) D. Landini, A. Maia, *Tetrahedron Lett.* **2005**, 46, 3961.
- [98] a) J. Jacquemin, M. F. Costa Gomez, P. Husson, V. Majer, *J. Chem. Thermodyn.* **2006**, 38, 490; b) J. Kumelan, A. Perez Salado Kamps, D. Tuma, G. Maurer, *J. Chem. Eng. Data* **2006**, 51, 1364; c) J. Huang, A. Riisager, P. Wasserscheid, R. Fehrmann, *Chem. Commun.* **2006**, 4027.
- [99] M. Costantini, V. A. Toussaint, A. Shariati, C. J. Peters, I. Kikic, *J. Chem. Eng. Data* **2005**, 50, 52.
- [100] a) J. K. Shah, E. J. Maginn, *J. Phys. Chem. B* **2005**, 109, 10395; b) X. Huang, C. J. Margulis, Y. Li, B. J. Berne, *J. Am. Chem. Soc.* **2005**, 127, 17842; c) C. Cadena, J. L. Anthony, J. K. Shah, T. I. Morrow, J. F. Brennecke, E. J. Maginn, *J. Am. Chem. Soc.* **2004**, 126, 5300; d) C. Hanke, R. M. Lynden-Bell, *J. Phys. Chem. B* **2003**, 107, 10873.
- [101] J. L. Anthony, E. J. Maginn, J. F. Brennecke, *J. Phys. Chem. B* **2002**, 106, 7315.
- [102] J. L. Anthony, E. J. Maginn, J. F. Brennecke, *J. Phys. Chem. B* **2001**, 105, 10942.
- [103] a) S. Wiegand, M. Kleemeier, J. M. Schröder, W. Schröder, H. Weingärtner, *Int. J. Thermophys.* **1994**, 15, 1045; b) L. Lachwa, J. Szydłowski, N. Najdanovic-Visak, L. P. N. Rebelo, K. R. Seddon, M. Nunes da Ponte, J. M. S. S. Esperança, H. J. R. Guedes, *J. Am. Chem. Soc.* **2005**, 127, 6542.
- [104] H. Weingärtner, T. Merkel, U. Maurer, J.-P. Conzen, H. Glasbrenner, S. Käshammer, *Ber. Bunsen-Ges.* **1991**, 95, 1579.
- [105] a) M. Wagner, O. Stanga, W. Schröder, *Phys. Chem. Chem. Phys.* **2003**, 5, 3943; b) M. Wagner, O. Stanga, W. Schröder, *Phys. Chem. Chem. Phys.* **2004**, 6, 4421.
- [106] H. Weingärtner, *J. Chem. Thermodyn.* **1997**, 29, 1409.
- [107] L. Cammarata, S. G. Kazarian, P. A. Salter, T. Welton, *Phys. Chem. Chem. Phys.* **2001**, 3, 5203.